

## Original Article

# Anti-tumor activity of chlorogenic acid by regulating the mTORC2 signaling pathway and disrupting F-actin organization

Shirui Tan<sup>1,2</sup>, Xiangshu Dong<sup>1</sup>, Dandan Liu<sup>1</sup>, Shumei Hao<sup>1</sup>, Feifei He<sup>1</sup>

<sup>1</sup>School of Agriculture, Yunnan University, Kunming 650091, China; <sup>2</sup>Center for Life Sciences, School of Life Sciences, Yunnan University, Kunming 650091, China

Received September 9, 2017; Accepted September 12, 2018; Epub May 15, 2019; Published May 30, 2019

**Abstract:** Chlorogenic acid (CGA), a plant-based dietary polyphenol exhibits potential anti-cancer capability. However, the precise molecular mechanisms remain to be elucidated. In the present study, the inhibitory effect of CGA on tumor cells was investigated in vitro and in vivo and its possible mechanisms involving filamentous actin (F-actin) organization was investigated. By cell viability, apoptosis, and cell cycle analysis, we demonstrate that CGA effectively inhibits tumor cell growth in vitro. Also, CGA treatment inhibits migration and invasive ability of cancer cells. Further studies revealed that CGA modulates mTORC2-associated signaling pathways with decreased phosphorylation of p-protein kinase C alpha (PKC $\alpha$ ), Akt, decreased expression of Rictor and F-actin which are known to activate cell growth and organize the actin cytoskeleton. Consistently, administration of CGA to mice bearing tumor cell-implanted xenografts also inhibited tumor growth in vivo. Collectively, these data suggest that the mTORC2/F-actin pathway is involved in CGA-induced tumor suppression. CGA might have the potential to become an anti-cancer agent.

**Keywords:** Chlorogenic acid, HepG2 cells, A549 cells, mTORC2, F-actin

## Introduction

Chlorogenic acid (CGA), a dietary polyphenol, is common in edible and medicinal plants and is formed by quinic acid and caffeic acid [1, 2]. Amount of studies on CGA demonstrate that it has a wide range of biological activities including inhibition of tumor cells [3-5]. However, its exact mechanism of anti-tumor activity is not fully understood. In order to better understand the anti-tumor activity of CGA, make better use of traditional Chinese medicine resources, and provide better drug candidates for cancer patients, we explored the anti-tumor mechanism using mouse liver and lung cancer models.

Epithelial-mesenchymal transition (EMT) is a decisive step that drives cancer cell invasion and metastasis [6-8]. Moreover, abnormal arrangement of cytoskeleton is closely associated with EMT and cancer progression [9, 10]. Recent reports have indicated that several anti-cancer drugs and potential therapeutic agents for cancer have important roles in inducing cytoskeleton redistribution and collapse in cancer cells [11, 12]. Dexamethasone could dis-

rupt cytoskeleton organization and inhibit migration of T47D human breast cancer cells by modulating the mTOR pathway [13]. Potential anticancer agents could induce apoptosis in DU145 prostate cancer cells by disrupting the F-actin organization [14]. Ferrocenyl-containing N-acetyl-2-pyrazolines efficiently inhibited human lung cancer growth by interfering with F-actin stress fiber polymerization [15]. Growth arrest specific 7C protein (GAS7) inhibited tumor metastasis by the hnRNP U/ $\beta$ -TrCP/ $\beta$ -catenin and N-WASP/FAK/F-actin pathways in lung cancer [16]. Furthermore, dynamic rearrangement of F-actin is required to maintain the antitumor effect of Trichostatin [17]. Altogether, these results have suggested that F-actin should be considered as a target for cancer treatment [18]. To the best of our knowledge, there have been no prior reports about the influence of CGA on the distribution of cytoskeleton.

The mechanistic target of rapamycin (mTOR) pathway plays pivotal roles in cell growth, proliferation, and survival [19] and is commonly activated in many cancers [20]. mTOR is a serine/threonine protein kinase that integrates

## Chlorogenic acid regulates F-actin organization

growth factor receptor signaling through mTORC1 and mTORC2 and mTORC1 is a validated cancer drug target [21]. However, the function of mTORC2 during cancer progression is less well understood compared to mTORC1 [22]. Emerging evidence from recent research has shown that mTORC2 also plays a very important role in cancer progression. Rictor, an mTORC2 subunit, is often found overexpressed in many gliomas. Moreover, forced overexpression of Rictor promotes activity of mTORC2 and endows cancer cells with increased proliferative and invasion potential [23-25]. Activation of mTORC2 is essential for keratinocyte survival and the early stages of skin tumorigenesis [26] and the development of prostate cancer in mice caused by the loss of tumor suppressor PTEN requires mTORC2 function [27]. Recent reports have shown that the Rictor-mTORC2 complex is important for organization of the actin cytoskeleton structure [28, 29]. However, whether CGA treatment could influence the signal pathway still remains elusive.

In our present study, the anti-tumor effect of CGA was investigated both in A549 and HepG2 cell lines using in vitro culture and in vivo xenograft nude mouse models to assess the potential mechanism of the protective role of CGA on tumor development.

### Materials and methods

#### *Cell treatment*

The A549 and HepG2 cell lines were purchased from the Shanghai Institute of Cell Biology (Shanghai, China). Cells were cultured in RPMI-1640 (A549) or DMEM (HepG2) medium supplemented with 10% (v/v) heat-inactivated fetal bovine serum (FBS) 100 mg/mL of streptomycin, and 100 U/mL of penicillin, and maintained at 37°C under 5% humidified CO<sub>2</sub>. For cell treatment, all cell lines were treated with CGA at a concentration of 5, 20, or 80 µM. For detecting cell viability, Cell Counting Kit (CCK-8) was used (Dojindo Laboratories, Japan).

#### *Flow cytometry*

Cells were harvested after treatments as indicated above, washed with cold PBS, and then processed for cell apoptosis and cell cycle analysis using flow cytometry. For apoptosis analysis, cells were harvested and washed twice

with PBS, and the Annexin-V/PI Kit (BMF500FI, eBioscience) was used according to guidelines from the manufacturer. For cell cycle analysis, briefly, the cells were fixed in 75% ethanol. The fixed cells were centrifuged at 800 rpm and washed with cold PBS twice. Propidium iodide (PI) staining solution (50 µg/ml final concentration; Beyotime Company, Shanghai, China) was added to the cells and incubated in the dark at 37°C for 30 min. The stained cells were collected using a BD FACS Calibur cytometer. Finally, all the data were analyzed using Flow Jo software (Tree Star, San Carlos, CA, USA).

#### *Wound healing and cell invasion assay*

Wound healing assays were carried out to evaluate the migration of cells under the treatment of CGA. A549 and HepG2 cells were seeded in six-well plates at  $1 \times 10^5$  per well in culture medium. Confluent monolayers were starved overnight and then a single scratch wound was created using a micropipette tip. Cell debris was washed away using PBS, and then they were supplemented with assay medium. Images were captured with a microscope using a 5 × objective at 24 h post-wounding.

The effect of CGA on A549 and HepG2 cell invasion was performed briefly as following: the cells were seeded into the top chambers of a 24-well Matrigel-coated polyethylene terephthalate membrane inserts with 8 µm pores (Millipore, Billerica, MA, USA) and treated with CGA at different concentration. The plates were coated with 10 µL of type I chamber of the Matrigel-coated transwell insert. The medium of the lower chambers contained 0.1 mg/mL bovine serum albumin as a chemoattractant. The cells were incubated at 37°C for 48 h. The cells that had invaded the outer surface of the membrane were fixed with methanol, and stained with hematoxylin and eosin, and photographed (CKX41, Olympus, Tokyo, Japan).

#### *Western blot*

Proteins were extracted using lysis buffer (50 mM Tris-Cl pH 8.0, 150 mM NaCl, 0.1% SDS, 0.02% NaN<sub>3</sub>, 100 mg/ml phenyl-methylsulfonyl fluoride (PMSF), 10 µg/mL aprotinin, 1 mg/ml Aprotinin, 1% Triton, 10 µg/mL leupeptin, 1 mM dithiothreitol, 1 mM paranitrophenyl phosphate, and 0.1 mM Na<sub>3</sub>VO<sub>4</sub>) and the protein concentration of each sample was detected using

## Chlorogenic acid regulates F-actin organization

the BCA protein assay kit (Pierce Chemical, Rockford, IL). Total lysates were resolved by 10% SDS-PAGE and transferred to nitrocellulose. Primary anti-human polyclonal antibodies are listed as follows: mTOR (1:2000 dilution; Abcam, ab2732), anti-phospho-mTOR (Ser2481) (1:1000 dilution; Cell Signaling Technology, 2974), anti-Akt (1:1000 dilution; Cell Signaling Technology, 4691), anti-phospho-Akt (Ser473) (1:2000 dilution; Cell Signaling Technology, 4060), anti-PKC $\alpha$  (1:1000 dilution; Cell Signaling Technology, 2056), anti-phospho-PKC $\alpha$  (1:1000 dilution; Santa Cruz, 12356), anti-Rictor (1:1000 dilution; Cell Signaling Technology, 2114) anti-F-actin (1:500 dilution Abcam, ab205) and GAPDH (1:1000 dilution; Thermo Fisher Scientific, MA5-15738-BTIN) the primary antibodies were detected by incubation with horseradish peroxidase (HRP)-conjugated anti-rabbit/mouse anti-body (1:2000 dilution; Beyotime). The densitometry software Quantity One v4.62 was used for protein expression analysis.

### *Xenograft mouse model*

6-7 week old female BALB/c nude mice were purchased from Guangdong Medical Lab Animal Center and treated in accordance with the Guide for the Care and Use of Laboratory Animals (National Institutes of Health, USA) and all manipulations were approved by the Yunnan University Animal Care Commission. For the xenograft,  $2 \times 10^6$  A549 or HepG2 cells were implanted into mice subcutaneously. When tumors became palpable, the mice were divided into 4 groups randomly (5 mice per group): group 1, vehicle control (treated with DMSO in saline); group 2 (50 mg/kg CGA); group 3 (100 mg/kg CGA); group 4 (200 mg/kg CGA). All treatments were done through intraperitoneal injection every two days for 4 weeks. The tumor volume was measured using a vernier caliper every 5 days and calculated as follows: volume (mm<sup>3</sup>) = length  $\times$  width  $\times$  width/2.

### *Immunofluorescence labeling and microscopy*

For the detection of F-actin distribution, cell lines were grown on cover slips and treated with increasing concentrations of CGA for 48 h. After the incubation, cells were rinsed in PBS and fixed with 4% paraformaldehyde for 1 h at RT. After rinsing, the cells were permeabilized with 0.2% triton X-100 containing PBS and were blocked before primary antibody incubation for

5 min with 1% BSA in PBS. Rinsed cells were labeled with F-actin by using phalloidin-conjugated to Alexa Fluor<sup>®</sup> 594 (5 U/ml; Invitrogen, Molecular Probes) for 1 h. Cells were washed four times with PBS, mounted with 0.5  $\mu$ g/ml 4, 6-diamidino-2-phenylindole (DAPI) containing 30% glycerol in PBS. The images were acquired using a fluorescence microscope (Olympus, Tokyo, Japan).

### *Immunohistochemistry of tumors*

Excised tumor tissues were fixed in 4% paraformaldehyde (PFA) and embedded in paraffin. Paraffin blocks were trimmed as necessary and cut at 5  $\mu$ m, and then serial sections of the embedded specimens were deparaffinized, rehydrated, and subjected to antigen retrieval. Then slides were incubated with anti-Ki-67 (Abcam, ab15580), anti-F-actin (Abcam, ab205) or anti-phospho-mTOR (Ser2481) (Cell Signaling Technology, 2974) (all these antibodies were used at a 1:100 dilution in PBS containing 1% FBS) for 2 h, followed by a biotinylated secondary antibody for 30 min, and then streptavidin-HRP for 20 min. Then slides were developed by incubation with the 3, 3'-diaminobenzidine (DAB) and the slides were counter stained with hematoxylin. The images were collected from five fields per section under 200  $\times$  magnifications.

### *Statistical analysis*

Data are presented as the mean  $\pm$  SD and analyzed using GraphPad Prism 5.0 software. Student's t-test was used to compare between two groups. One-way ANOVA analysis of variance was used to compare among three or more groups. A value of  $P < 0.05$  was considered statistically significant. Experiments were performed at least three times and representative experiments are shown.

## Results

### *CGA inhibits tumor cell growth in vitro*

The anti-tumor activity of CGA was tested on A549 and HepG2 cell lines. The cells were treated with CGA (0, 5, 20, or 80  $\mu$ M) for 48 h and cell viability was determined by the CCK-8 assay. Briefly, after 48 h culture, the medium were changed to fresh medium with 10% CCK8 (Dojindo Laboratories, Japan). The absorption data at 450 nm were detected 30 minutes

## Chlorogenic acid regulates F-actin organization

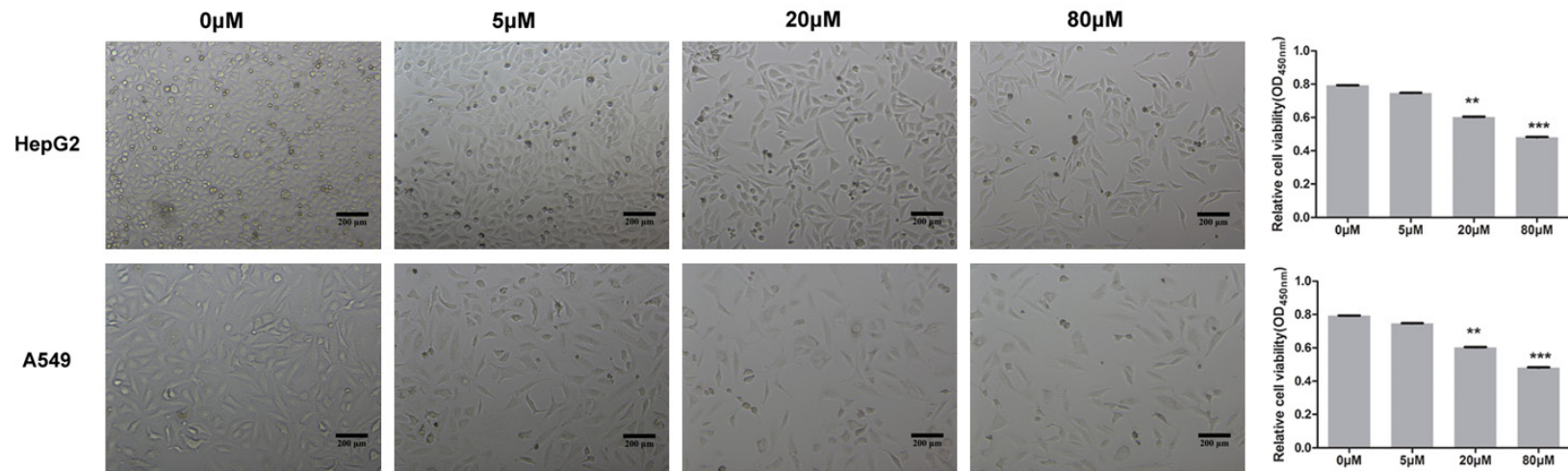


**Figure 1.** CGA inhibits tumor cell growth *in vitro*. Cancer cell lines were treated with CGA at (5, 20, or 80 μM) for 48 h. Cell viabilities were examined by CCK-8 assay. Representing figures of cells after culture were shown in the left and cell viability determined by absorption data at 450 nm was shown in the right. Bar = 200 μm. Quantitative data are presented as the mean ± SD from three independent experiments. \*P < 0.05; \*\*P < 0.01; \*\*\*P < 0.001.

## Chlorogenic acid regulates F-actin organization

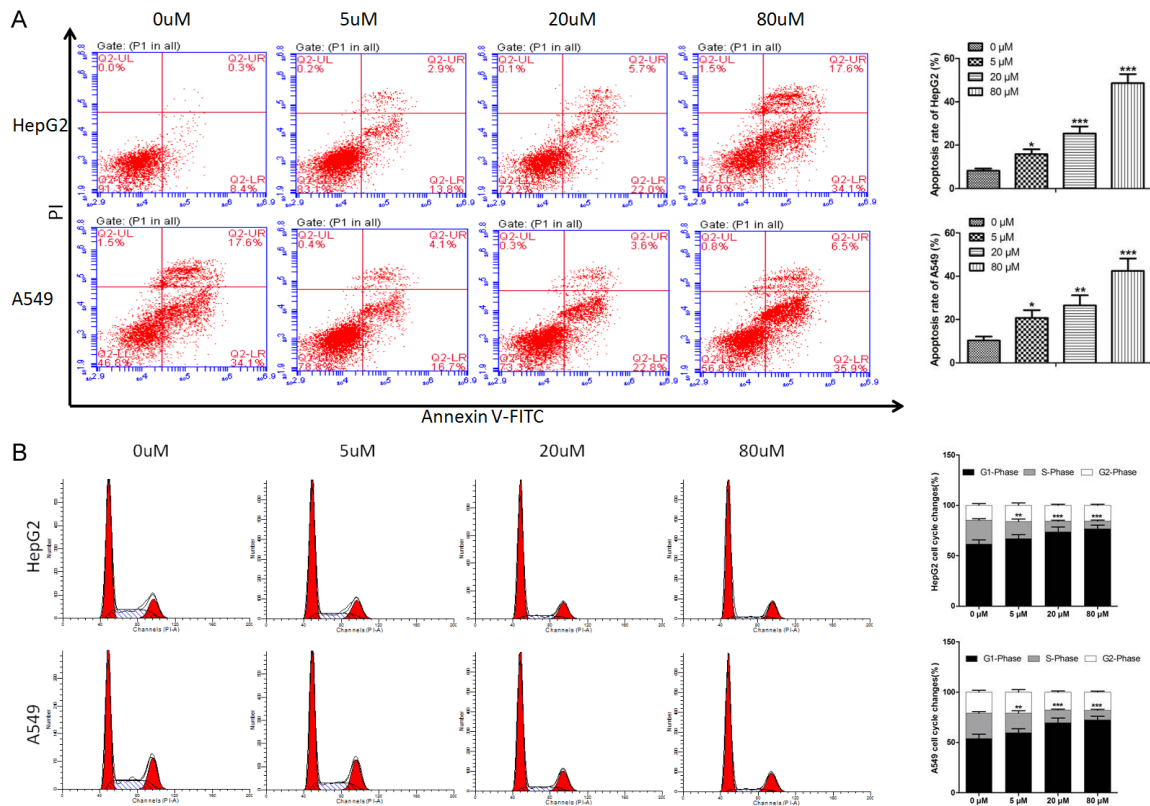


**Figure 2.** CGA induced cell apoptosis and cell cycle blockage *in vitro*. Cancer cell lines were treated with CGA at indicated concentration and time. Cell apoptosis level (A) and cell cycle states (B) were determined by flow cytometry and analyzed by flowJo. Quantitative data are presented as the mean  $\pm$  SD from three independent experiments. \* $P < 0.05$ ; \*\* $P < 0.01$ ; \*\*\* $P < 0.001$ .

using microplaterereader. As shown in **Figure 1**, both HepG2 and A549 tumor cells treated with CGA showed decreased cell viability in a dose dependent manner compared to vehicle treated cells, suggesting CGA has an inhibitory effect on tumor cells.

### *CGA induces tumor cell apoptosis and cell cycle blockage in vitro*

To further confirm the antitumor ability of CGA, studies were conducted to examine the level of apoptosis and cell cycle status. As shown in **Figure 2A**, cells treated with CGA have increased apoptosis and a blockage of the cell cycle in the G1 to S phase in a dose-dependent manner (**Figure 2B**).

### *CGA inhibits cell migration and invasion ability of cancer cells*

As cell migration is an essential step for cancer metastasis, we next examined the inhibition

ability of CGA on cell migration on the two cell lines using scratch wound healing assays. The results in **Figure 3A** show that untreated A549 and HepG2 cells covered more damaged area at 24 h compared with the cells treated with CGA at 5, 20, or 80  $\mu$ M. Also, compared with control groups, the distance of the scratch wound in the CGA treated group was significantly larger. In addition, in order to study whether CGA disturbs the invasiveness of malignant cancer cells, Matrigel invasion assay was conducted. The results showed that CGA inhibited cancer cells moving into the Matrigel chamber in a dose-dependent manner (**Figure 3B**). These results indicate that CGA can inhibit the migration and invasion of cancer cells.

### *CGA led to F-actin disruption in vitro*

Previous results show that a number of cytoskeleton changes could lead to cell apoptosis and cell cycle disruption [30] and could lead to

## Chlorogenic acid regulates F-actin organization

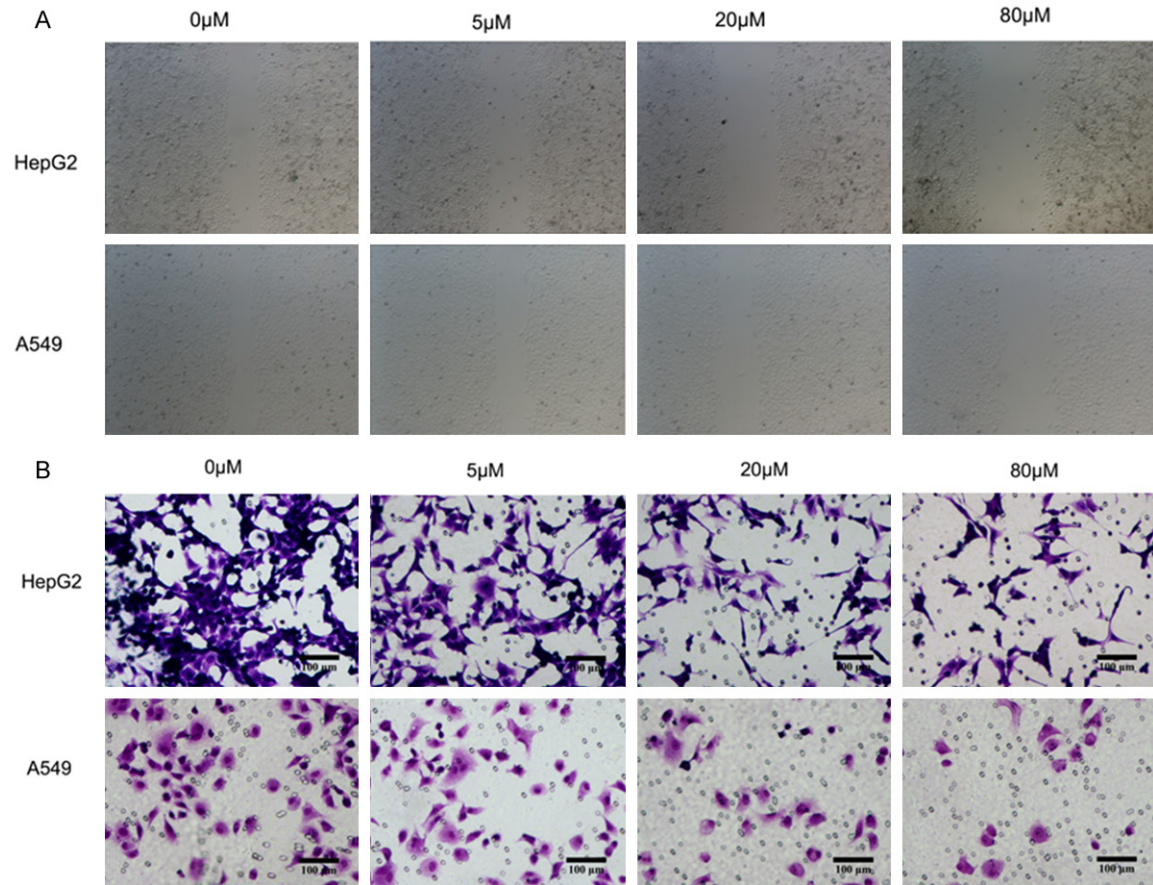


**Figure 3.** CGA decreases cell motility as assessed by wound healing assay. Cells cultured in 12 well plates were monitored for their ability to migrate into the created wound gap. The wound gap was photographed 24 h after created. The wound healing images demonstrated that A549 and HepG2 cells treated with CGA migrated much slower than vector control cells ( $\times 40$ ) (A). Cells were treated for 48 h with of CGA at indicated concentrations and the cell invasion assay (B) was performed in a Matrigel-coated chamber system as described in Materials and Methods. Bar = 100  $\mu\text{m}$ . Representative photographs of three independent experiments were shown.

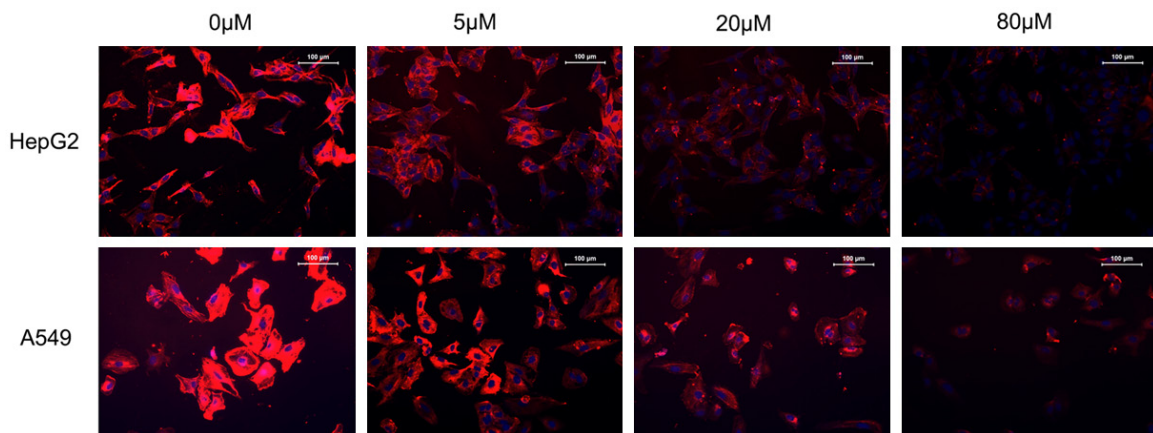


**Figure 4.** CGA led to F-actin disruption *in vitro*. CGA-induced changes in F-actin distribution following 48 h of exposure in A549 and HepG2 cells. A549 and HepG2 cells plated on cover slips were treated with increasing concentrations of CGA. F-actin (red) were stained with Alexa Fluor® 594 phalloidin and DAPI for the nucleus (blue). Cells were imaged at a  $\times 60$  objective at identical exposure settings with immunofluorescence microscope. The bar indicates 100  $\mu\text{m}$ .

# Chlorogenic acid regulates F-actin organization

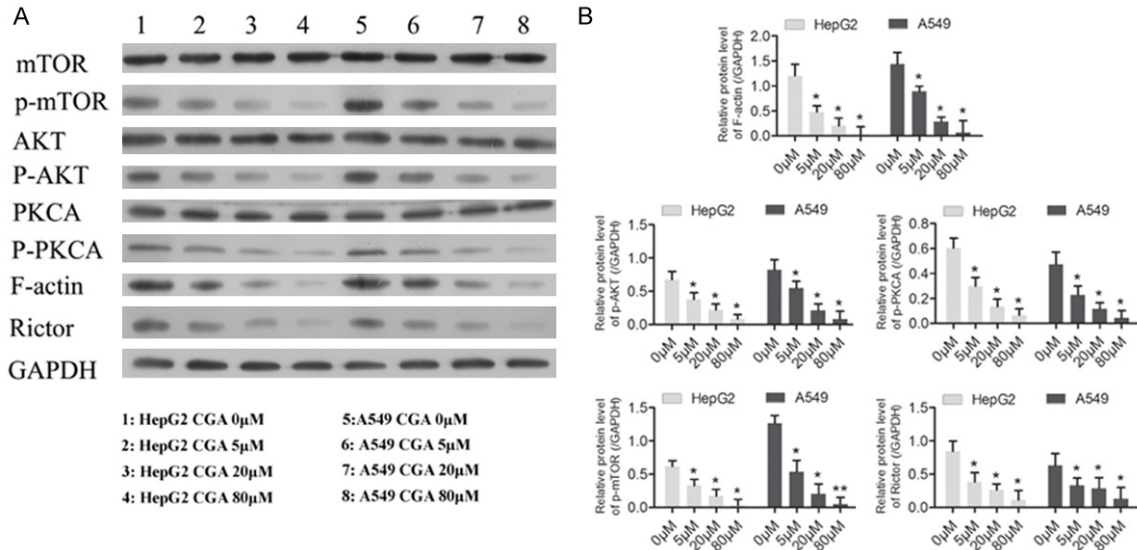


**Figure 5.** CGA regulates mTORC2 activity through Rictor expression. A549 and HepG2 cells were treated for 24 h with increasing concentrations of CGA and the expression of mTORC2 signaling-related proteins (PKC $\alpha$ , p-PKC $\alpha$ , Akt, p-Akt, Rictor, and F-actin) were measured by Western blot analysis (A) and the relative expression level of p-PKC $\alpha$ , p-Akt, Rictor, p-mTORC2 and F-actin were quantified using Quantity One (B). \*P < 0.05.

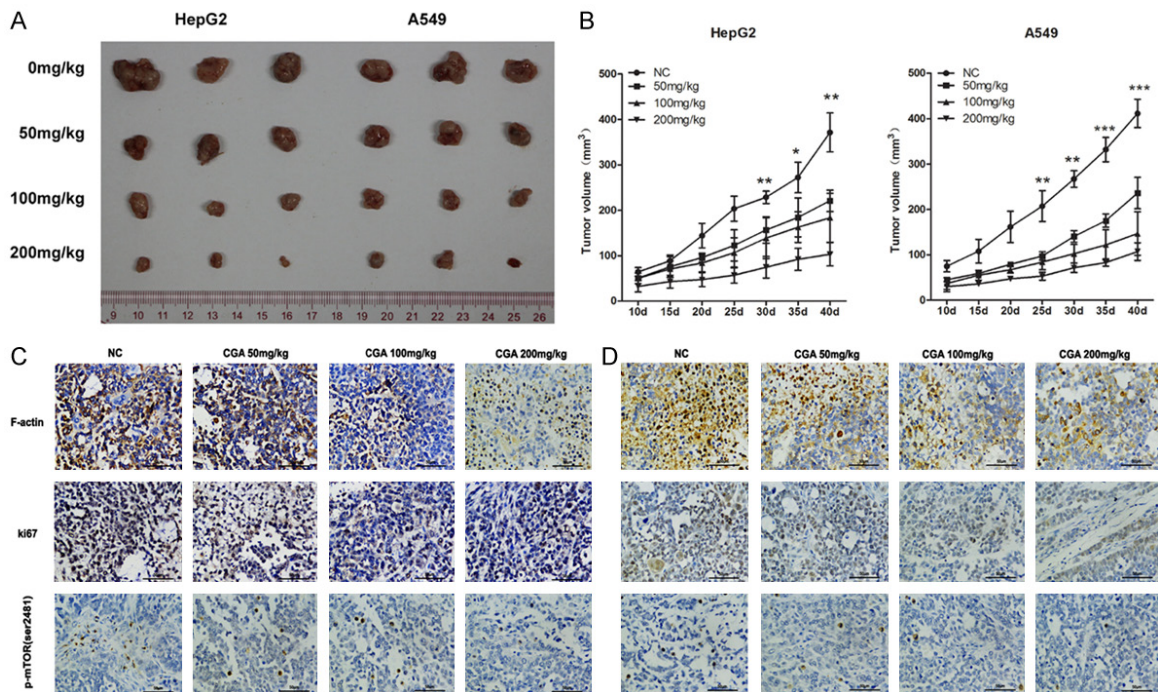


**Figure 6.** CGA administration suppresses growth of xenografts *in vivo*. Female Balb/c nude mice bearing A549 and HepG2 xenografts were administrated with CGA or DMSO through intraperitoneal injection every two days for 4 weeks. Tumor volume (A) was recorded every 5 days. Three out of five representing tumor from each group was show after sacrifice (B). Data are shown as mean  $\pm$  se M (n = 5). The Ki67 (indicates by brown color) expression level, F-actin (brown color) expression level, and phosphorylation of mTORC2 (p-mTOR2481) (brown color) was measured by immunohistochemistry (C, D) and the nuclear is counterstained by hematoxylin (Blue). \*P < 0.05, \*\*P < 0.01, control group compared with all groups treated with CGA. The bar indicates 50  $\mu$ m.

## Chlorogenic acid regulates F-actin organization

inhibition of tumor progression [13]. F-actin has been proven to be one of the very important targets of anti-tumor agents [17, 18]. Therefore, we wanted to know whether the inhibitory activity of CGA on tumor progression was associated with F-actin organization. To do this, immunofluorescence labeling to stain filamentous F-actin was performed to determine the intracellular cytoskeletal actin distribution. As shown in **Figure 4**, distinct changes in cell morphology and organization of F-actin filaments was observed in cells treated with increasing doses of CGA: randomly distributed F-actin condensation emerged in the cells treated with CGA, while vehicle treated cells developed actin cytoskeleton with clearly visible structure. Many cells reduced their volume and intercellular contacts which had fewer actin fibers and disrupted actin organization.

### *CGA treatment also downregulates mTORC2 activity*

Previous research has shown that inhibition of the Rictor-mTORC2 signal pathway impairs the actin cytoskeletal structure [28, 29]. Therefore, we wanted to know whether the mTORC2 signal pathway was also interrupted after CGA treatment. Western blot was carried out to determine the activation level of the mTORC2 signal pathway. Ser473 of Akt is phosphorylated by mTORC2 [31] and PKC $\alpha$  is also a substrate of mTORC2 [28, 29]. PKC $\alpha$  is phosphorylated at Ser657 by mTORC2 and regulates actin remodeling. Here, we investigated whether CGA regulates pPKC $\alpha$  S657 and pAkt Ser473 through mTORC2. We observed the relative protein expression level of PKC $\alpha$ , AKT and mTOR is not significantly different between control and CGA treated group (**Figure 5A** and analysis data not shown). While in CGA treated A549 and HepG2 cells, both the pPKC $\alpha$  (Ser657) and pAkt (S473) levels were reduced in a dose dependent manner and the expression level of F-actin was also significantly reduced in CGA treated cells compared to control cells (**Figure 5A, 5B**). Consistent with this result, Rictor, an important component of the mTORC2 complex, was also significantly reduced in CGA treated cells (**Figure 5A, 5B**). These results suggested that CGA leads to F-actin disruption, and probably the down regulation of the Rictor-mTORC2 signal pathway is involved in this disruption.

### *CGA administration suppresses growth of xenografts in vivo*

In order to confirm whether CGA could exert an inhibitory effect on tumor progression *in vivo*, we conducted experiments using A549 and HepG2 xenografts in a nude mouse model. Tumor volume was measured every 5 days for 8 weeks. After 4 weeks of treatment, mice were sacrificed for experiments. As shown in **Figure 6A, 6B**, CGA treatment, especially at high dose, did markedly suppress the growth of both A549 and HepG2 tumors *in vivo*. In addition, we also examined the expression level of Ki67, a tumor proliferation marker by immunohistochemistry assay. As the results (**Figure 6C, 6D**) show, after CGA treatment, ki67 positive proliferating cells are significantly reduced compared to control group. Moreover, consistent with our *in vitro* results, the immunohistochemistry staining results of F-actin and mTORC2 (**Figure 6C, 6D**) confirmed CGA treatment disrupted the expression pattern of F-actin and inhibited phosphorylation of mTORC2. Taken above together, these findings demonstrate that CGA inhibits tumor growth both *in vivo* and *in vitro* and disruption of F-actin organization and decreased mTORC2 signal activity contributes to its antitumor effect.

## Discussion

Natural products have been developed as anti-cancer agents in the clinical setting for a long time [32]. The antitumor effect of CGA on tumor cells has been studied in many human cancer cells [33-35], but the underlying mechanism is still unclear. Therefore, the present study focused on A549 and HepG2 cells *in vitro* and *in vivo* to study the antitumor role of CGA. We found that CGA had a strong cytotoxic activity toward both A549 and HepG2 cells in a dose-dependent manner. In addition, CGA could also lead to tumor cell apoptosis, cell cycle arrest, and decreased cell migration and invasion ability. Furthermore, we confirmed the *in vivo* antitumor capability of CGA in nude mice bearing tumor xenografts. Importantly, we found that, CGA could lead to F-actin disruption in tumor cells and that this disruption was partially due to decreased rictor-mTORC2 complex activity. This study suggests that CGA disrupt the organization of F-actin, probably through inhibiting the mTORC2 signaling pathway.

## Chlorogenic acid regulates F-actin organization

Previous results have shown that CGA administration could lead to tumor cell apoptosis and cell cycle arrest [36]. Consistent with their results, we also find that CGA treatment could lead to reduced cell viability, increased apoptosis, and cell cycle arrest. Also, we found that CGA treatment reduced the cell migration and invasion ability which were identical to a prior report on the investigation of anti-invasive properties of derivatives from cinnamic acid on adenocarcinoma cells [35]. Since the cytoskeleton exerts important roles in tumor cell migration and invasion [9, 10] and recent research has proven that targeting F-actin origination could control tumor cell migration [17, 37-39]. Therefore, we investigated the influence of CGA on F-actin organization, and for the first time report that CGA treatment could lead to F-actin disruption in tumor cells.

The activation of the mTOR signal pathway, which including mTORC1 and mTORC2, has important roles in cancer progression [19, 20, 22], and recent reports have shown that the mTORC2 signaling pathway can control the actin cytoskeleton [23, 28, 40]. However, no report has shown that CGA could influence mTOR activation. Here, we show for the first time that CGA could lead to decreased mTORC2 activation, which was demonstrated by less phosphorylation of mTORC2 and downstream pPKC $\alpha$  and pAkt signals. Importantly, these phenomena were due to decreased expression of Rictor, an essential component of the mTORC2 complex. However, how CGA treatment decreased the expression level of Rictor and the mechanism involved in this regulation needs further investigation.

In conclusion, we describe the anti-tumor effect of CGA and show that they are, in part, due to the disruption of F-actin organization pattern and inhibition of mTORC2 signaling.

### Acknowledgements

This work was supported by the Scientific Research Fund of Yunnan Provincial Education Department of China (Grant No. 2016zzx007 and 2016zzx009), scientific research fund of Yunnan Province (Grant No. 2017FB108).

### Disclosure of conflict of interest

None.

**Address correspondence to:** Drs. Shumei Hao and Feifei He, School of Agriculture, Yunnan University, No. 2, Cuihu North Road, Kunming 650091, China. E-mail: haosm@sina.com (SMH); Tel: +86-871-65031539; Fax: +86-871-65031539; E-mail: hefeifei@ynu.edu.cn (FFH)

### References

- [1] Huang MT, Wong CQ, Conney AH. Inhibitory effect of curcumin, chlorogenic acid, caffeic acid, and ferulic acid on tumor promotion in mouse skin by 12-O-tetradecanoylphorbol-13-acetate. *Cancer Res* 1988; 48: 5941-6.
- [2] Farah A, Monteiro M, Donangelo CM and Lafay S. Chlorogenic acids from green coffee extract are highly bioavailable in humans. *J Nutr* 2008; 138: 2309-2315.
- [3] Kang TY, Yang HR, Zhang J, Li D, Lin J, Wang L and Xu X. The studies of chlorogenic Acid anti-tumor mechanism by gene chip detection: the immune pathway gene expression. *J Anal Methods Chem* 2013; 2013: 617243.
- [4] Feng R, Lu Y, Bowman LL, Qian Y, Castranova V and Ding M. Inhibition of activator protein-1, NF-kappaB, and MAPKs and induction of phase 2 detoxifying enzyme activity by chlorogenic acid. *J Biol Chem* 2005; 280: 27888-27895.
- [5] Lee WJ and Zhu BT. Inhibition of DNA methylation by caffeic acid and chlorogenic acid, two common catechol-containing coffee polyphenols. *Carcinogenesis* 2006; 27: 269-277.
- [6] Acloque H, Adams MS, Fishwick K, Bronner-Fraser M and Nieto MA. Epithelial-mesenchymal transitions: the importance of changing cell state in development and disease. *J Clin Invest* 2009; 119: 1438-1449.
- [7] Nieto MA. Epithelial-Mesenchymal Transitions in development and disease: old views and new perspectives. *Int J Dev Biol* 2009; 53: 1541-1547.
- [8] Thiery JP, Acloque H, Huang RY and Nieto MA. Epithelial-mesenchymal transitions in development and disease. *Cell* 2009; 139: 871-890.
- [9] Pandey P, Rachagani S, Das S, Seshacharyulu P, Sheinin Y, Naslavsky N, Pan Z, Smith BL, Peters HL, Radhakrishnan P, McKenna NR, Giridharan SS, Haridas D, Kaur S, Hollingsworth MA, MacDonald RG, Meza JL, Caplan S, Batra SK and Solheim JC. Amyloid precursor-like protein 2 (APLP2) affects the actin cytoskeleton and increases pancreatic cancer growth and metastasis. *Oncotarget* 2015; 6: 2064-2075.
- [10] Sun BO, Fang Y, Li Z, Chen Z and Xiang J. Role of cellular cytoskeleton in epithelial-mesenchymal transition process during cancer progression. *Biomed Rep* 2015; 3: 603-610.

## Chlorogenic acid regulates F-actin organization

- [11] Lockett S, Verma C, Brafman A, Gudla P, Nandy K, Mimaki Y, Fuchs PL, Jaja J, Reilly KM, Beutler J and Turbyville TJ. Quantitative analysis of F-actin redistribution in astrocytoma cells treated with candidate pharmaceuticals. *Cytometry A* 2014; 85: 512-521.
- [12] Wang H, Zhang HM, Yin HJ, Zheng LQ, Wei MQ, Sha H and Li YX. Combination of a novel photosensitizer DTPP with 650 nm laser results in efficient apoptosis and cytoskeleton collapse in breast cancer MCF-7 cells. *Cell Biochem Biophys* 2014; 69: 549-554.
- [13] Meng XG and Yue SW. Dexamethasone disrupts cytoskeleton organization and migration of T47D human breast cancer cells by modulating the AKT/mTOR/RhoA pathway. *Asian Pac J Cancer Prev* 2015; 15: 10245-10250.
- [14] Korkmaz M, Avci CB, Gunduz C, Aygunes D and Erbaykent-Tepedelen B. Disodium pentaborate decahydrate (DPD) induced apoptosis by decreasing hTERT enzyme activity and disrupting F-actin organization of prostate cancer cells. *Tumour Biol* 2014; 35: 1531-1538.
- [15] Bostancioglu RB, Demirel S, Turgut Cin G and Koparal AT. Novel ferrocenyl-containing N-acetyl-2-pyrazolines inhibit in vitro angiogenesis and human lung cancer growth by interfering with F-actin stress fiber polymerization. *Drug Chem Toxicol* 2013; 36: 484-495.
- [16] Tseng RC, Mao JS, Tsai CD, Wu PC, Lin CJ, Lu YL, Liao SY, Cheng HC, Hsu HS, Wang YC. Growth-arrest-specific 7c protein inhibits tumor metastasis via the N-WASP/FAK/F-actin and hnRNP U/ $\beta$ -TrCP/ $\beta$ -catenin pathways in lung cancer. *Oncotarget* 2015; 6:44207-15.
- [17] Yang DH, Lee J, Moon EY. Dynamic rearrangement of F-actin is required to maintain the antitumor effect of trichostatin A. *PLoS One* 2014; 9: e97352.
- [18] Martin SK, Kamelgarn M and Kyprianou N. Cytoskeleton targeting value in prostate cancer treatment. *Am J Clin Exp Urol* 2014; 2: 15-26.
- [19] Hung CM, Garcia-Haro L, Sparks CA and Guertin DA. mTOR-dependent cell survival mechanisms. *Cold Spring Harb Perspect Biol* 2012; 4.
- [20] Perl A. mTOR activation is a biomarker and a central pathway to autoimmune disorders, cancer, obesity, and aging. *Ann N Y Acad Sci* 2015; 1346: 33-44.
- [21] Laplante M and Sabatini DM. mTOR signaling in growth control and disease. *Cell* 2012; 149: 274-293.
- [22] Masui K, Cavenee WK and Mischel PS. mTORC2 in the center of cancer metabolic reprogramming. *Trends Endocrinol Metab* 2014; 25: 364-373.
- [23] Masri J, Bernath A, Martin J, Jo OD, Vartanian R, Funk A and Gera J. mTORC2 activity is elevated in gliomas and promotes growth and cell motility via overexpression of rictor. *Cancer Res* 2007; 67: 11712-11720.
- [24] Hietakangas V and Cohen SM. TOR complex 2 is needed for cell cycle progression and anchorage-independent growth of MCF7 and PC3 tumor cells. *BMC Cancer* 2008; 8: 282.
- [25] Chantaravisoot N, Wongkongkathep P, Loo JA, Mischel PS and Tamanoi F. Significance of filamentin a in mTORC2 function in glioblastoma. *Mol Cancer* 2015; 14: 127.
- [26] Carr TD, Feehan RP, Hall MN, Ruegg MA and Shantz LM. Conditional disruption of rictor demonstrates a direct requirement for mTORC2 in skin tumor development and continued growth of established tumors. *Carcinogenesis* 2015; 36: 487-497.
- [27] Guertin DA, Stevens DM, Saitoh M, Kinkel S, Crosby K, Sheen JH, Mullholland DJ, Magnuson MA, Wu H and Sabatini DM. mTOR complex 2 is required for the development of prostate cancer induced by Pten loss in mice. *Cancer Cell* 2009; 15: 148-159.
- [28] Jacinto E, Loewith R, Schmidt A, Lin S, Ruegg MA, Hall A and Hall MN. Mammalian TOR complex 2 controls the actin cytoskeleton and is rapamycin insensitive. *Nat Cell Biol* 2004; 6: 1122-1128.
- [29] Sarbassov DD, Ali SM, Kim DH, Guertin DA, Latek RR, Erdjument-Bromage H, Tempst P and Sabatini DM. Rictor, a novel binding partner of mTOR, defines a rapamycin-insensitive and raptor-independent pathway that regulates the cytoskeleton. *Curr Biol* 2004; 14: 1296-1302.
- [30] Kilmartin JV and Adams AE. Structural rearrangements of tubulin and actin during the cell cycle of the yeast *Saccharomyces*. *J Cell Biol* 1984; 98: 922-933.
- [31] Sarbassov DD, Guertin DA, Ali SM and Sabatini DM. Phosphorylation and regulation of Akt/PKB by the rictor-mTOR complex. *Science* 2005; 307: 1098-1101.
- [32] DeCorte BL. Underexplored opportunities for natural products in drug discovery. *J Med Chem* 2016; 59: 9295-9304.
- [33] Yang JS LC, Ma YS, Weng SW, Tang NY, Wu SH, Ji BC, Ma CY, Ko YC, Funayama S, Kuo CL. Chlorogenic acid induces apoptotic cell death in U937 leukemia cells through caspase- and mitochondria-dependent pathways. *In Vivo* 2012; 26: 8.
- [34] Yan Y, Li J, Han J, Hou N, Song Y and Dong L. Chlorogenic acid enhances the effects of 5-fluorouracil in human hepatocellular carcinoma cells through the inhibition of extracellular signal-regulated kinases. *Anticancer Drugs* 2015; 26: 540-546.
- [35] Tsai CM, Yen GC, Sun FM, Yang SF and Weng CJ. Assessment of the anti-invasion potential and mechanism of select cinnamic acid deriv-

## Chlorogenic acid regulates F-actin organization

- atives on human lung adenocarcinoma cells. *Mol Pharm* 2013; 10: 1890-1900.
- [36] Liu YJ, Zhou CY, Qiu CH, Lu XM and Wang YT. Chlorogenic acid induced apoptosis and inhibition of proliferation in human acute promyelocytic leukemia HL60 cells. *Mol Med Rep* 2013; 8: 1106-1110.
- [37] Aggarwal S, Singh M, Kumar A and Mukhopadhyay T. SRD5A2 gene expression inhibits cell migration and invasion in prostate cancer cell line via F-actin reorganization. *Mol Cell Biochem* 2015; 408: 15-23.
- [38] Kang JI, Hong JY, Lee HJ, Bae SY, Jung C, Park HJ and Lee SK. Anti-tumor activity of Yuanhuacine by Regulating AMPK/mTOR signaling pathway and actin cytoskeleton organization in non-small cell lung cancer cells. *PLoS One* 2015; 10: e0144368.
- [39] Yasuda K, Takahashi M and Mori N. Mdm20 modulates actin remodeling through the mTORC2 pathway via its effect on rictor expression. *PLoS One* 2015; 10: e0142943.
- [40] Huang W, Zhu PJ, Zhang S, Zhou H, Stoica L, Galiano M, Krnjevic K, Roman G and Costamattioli M. MTORC2 controls actin polymerization required for consolidation of long-term memory. *Nat Neurosci* 2013; 16: 441-448.